Free-Form Deformation of Solid Models in CSR

K.C. Hui and C.F. Lai

Department of Automation and Computer-Aided Engineering,
The Chinese University of Hong Kong, Shatin, Hong Kong.
e-mail: kchui@acae.cuhk.edu.hk

Abstract

Existing free-form deformation (FFD) techniques deform an object by deforming the space enclosing the object. Points on the object are thus deformed relative to the undeformed space (or world space). The deformed object is visualized by sampling points on the object surfaces, or by approximating the object with a polyhedral model. This provides good visual effect for the deformed objects. However, the deformed solid is represented in terms of the lattice of the FFD and the undeformed solid. There is no precise explicit representation of the deformed object so that existing solid modeling techniques, such as Boolean operations, on the deformed object may not be applied. This paper is concerned with the techniques of applying free-form deformation on solid models represented by the Constructive Shell Representation (CSR). By applying free-form deformation on the surface points of the trunctets of a CSR object so that the vertices and the quadric patch polynomial of the trunctets are changed, the shape of the object can be modified. This technique can be used to deform globally smooth solid models or general solid models with sharp edges. The deformation can be applied either globally or locally. Techniques for the deformation are discussed in detail. Experiments are conducted and the results are also presented.

1. Introduction

Despite the popularity of the free-form deformation (FFD) techniques [1-5] for generating special effects in graphics and animations, its use as a modeling tool has not been fully explored. This is a result of the fact that the deformed object is not converted to an existing object representation scheme. For instance, solid objects represented in Boundary representation (B-rep) or Constructive Solid Geometry (CSG) can be deformed using the FFD techniques. However, further operations such as Boolean operations on the deformed object may not be performed since the deformed object is not converted to a B-rep or CSG model.

In order to allow solid operations to be performed on FFD deformed solids, a proper representation scheme for solid model, especially free-form objects, is required [6]. A popular approach is to represent free-form surfaces as parametric patches of high degree in B-rep [7-9]. This technique is very successful as far as design and rendering are concerned. However, manipulating and reasoning about physical objects with parametric patches poses fundamental difficulties. For instance, the difficulty in evaluating and representing intersections of parametric patches has been a major problem in the development of solid modeling systems based on parametric patches.

For objects represented in CSG, a fundamental problem that prohibited the use of FFD is the possible change of surface type as a result of the deformation. For example, a block may be bended so that the planar surfaces of the block will become quadrics or higher order surfaces. A number of different approaches have been proposed for incorporating freeform surfaces in CSG objects [10-13]. Among these approaches, the Constructive Shell Representation (CSR) proposed by J. Menon [13] seems to be most promising. The CSR allows freeform objects to be represented with low order implicit surfaces which is an essential feature in a CSG modeler. The CSR approach thus provides an attractive solution to the problem.

In this paper, CSR is adopted for representing solid objects. This allows CSG models to be deformed using FFD while existing modeling techniques can be applied.

2. Free-Form Deformation and the CSR Solid Models

The free-form deformation technique (FFD) [1] deforms an object by enclosing the object in a parallelepiped region defined with a lattice of control points. Manipulating the control points of the lattices deforms the parallelepiped region and hence the enclosed object.

A freeform deformation can thus be considered as a mapping $F: E^3 \rightarrow E^3$, that transforms every point of an object S to the deformed object F(S). Since the deformation can be applied to any point of an object, the technique can be applied on objects irrespective of their representation for generating a set of points on the deformed object. However, to allow further operations on the deformed objects, a conversion of the deformed points to entities of the underlying representation is required.

Using Constructive Shell Representation, a free-form solid S is represented as the union of a set of trunctets T_i and a polyhedron core H. Each trunctet is a tetrahedron truncated by an algebraic surface interpolating two or three vertices of the tetrahedron, i.e.

$$S = H \cup O \cup I, \qquad (2)$$

where $I = \bigcup_0^n I_i$ is the set of inner trunctets, and $O = \bigcup_0^n O_i$ is the set of outer trunctets.

Figure 1a shows a sectional view of a CSR object. Applying freeform deformation to the solid S may result in some inner trunctets becoming outer trunctets or vice versa. This may require the polyhedron core to be modified as the trunctets are being deformed. An alternative is adopted. In this approach S is represent as

$$S = H \cup O - N \qquad (3)$$

where $N = \bigcup_0^n N_i$ is the set of depression trunctets as shown in Figure 1b.

Define the deformation functions F_C, and F_T for the deformation of the polyhedron core and a trunctet respectively as follow.

Definition 1 Deformation of polyhedron core
Given a polyhedron core H with vertices $\mathbf{V}_i$, of an object S, and a freeform deformation F, the freeform deformed polyhedron core F_C(H) is the polyhedron with vertices $F(\mathbf{V}_i)$ and having the same topology (edge connectivity) as H.

Definition 2 Deformation of trunctet
Given a trunctet T with an algebraic patch A interpolating the tetrahedron base vertices $\mathbf{V}_i$, i = 1 … n, n = 2 or 3, and a freeform deformation F, the deformed trunctet F_T(T) is the trunctet with the patch F(A) interpolating the base vertices $F(\mathbf{V}_i)$.

A freeform deformed object S can thus be expressed as

$$F(\mathrm{S}) = F_C(\mathrm{H}) \cup \mathrm{O'} - \mathrm{N'} \qquad (4)$$

where O' and N' are respectively, the set of outer and depression trunctets in the deformed solid.

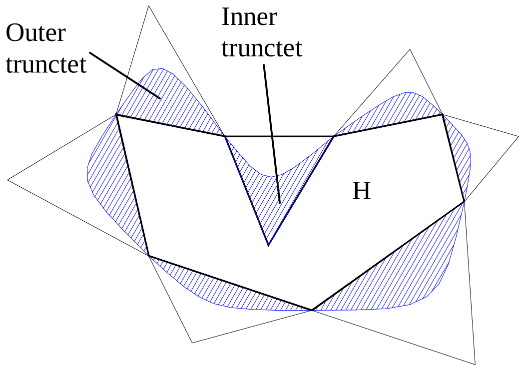

(a)

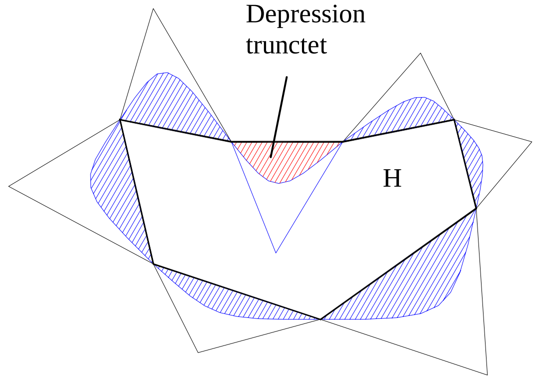

(b)

Figure 1 Two approaches for modelling a solid in CSR

In the approach proposed by J.P. Menon [13], two-sided gaps (Figure 2) may exist between adjacent trunctets in the construction of a free-form solid using trunctets. A smooth free-form object is obtained by filling the gaps with additional *blend-patches* that satisfy inter-patch continuity conditions [14]. The same approach will be applied in constructing the deformed model. The rest of the paper will thus focus on the deformation of a 3-sided trunctet.

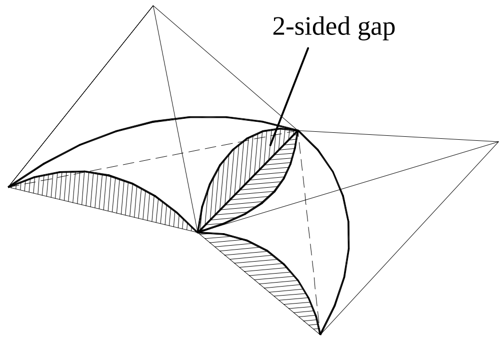

Figure 2 A 2-sided gap

3. Deformation of a Trunctet

A major concern in the deformation of a trunctet is the deformation of the algebraic patch of a trunctet. In this paper, quadric algebraic patch is adopted. Using Gua's approach [14], a quadric algebraic patch interpolating three vertices of a trunctet is defined as

$$a_b(s,t,u,v) = w_{2000}s^2 + w_{0200}t^2 + w_{0020}u^2 + w_{0002}v^2 + 2w_{1100}st + 2w_{1001}sv + 2w_{0011}uv + 2w_{0110}tu + 2w_{1010}su + 2w_{0101}tv = 0 \quad (5)$$

where s, t, u and v are barycentric coordinates relative to the vertices of the tetrahedron, w_{ijk} are weights associated with the control points on a trunctet (Figure 3).

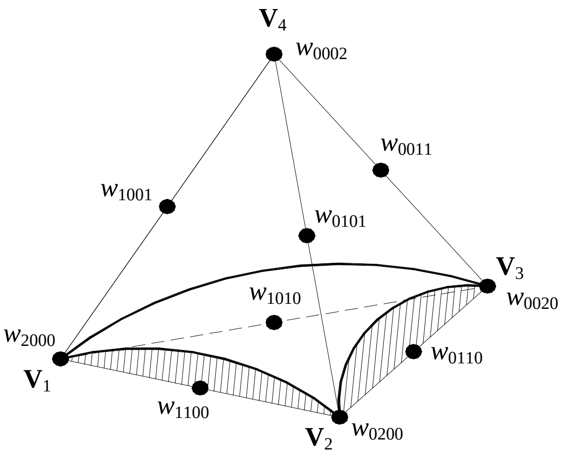

Figure 3 The weights and control points on a trunctet

The weights of a trunctet are determined by the surface normals $\mathbf{n}_i$ at the base vertices of the tetrahedron as given by the following equations [14].

$$\left.\begin{aligned} w_{1100} &= \frac{1}{2}(\mathbf{V}_2 - \mathbf{V}_1)\bullet\mathbf{n}_1 \\ w_{1010} &= \frac{1}{2}(\mathbf{V}_3 - \mathbf{V}_1)\bullet\mathbf{n}_1 \\ w_{1001} &= \frac{1}{2}(\mathbf{V}_4 - \mathbf{V}_1)\bullet\mathbf{n}_1 \end{aligned}\right\} \quad (6a)$$

$$\left.\begin{aligned} w_{1100} &= \frac{1}{2}(\mathbf{V}_1 - \mathbf{V}_2)\bullet\mathbf{n}_2 \\ w_{0110} &= \frac{1}{2}(\mathbf{V}_3 - \mathbf{V}_2)\bullet\mathbf{n}_2 \\ w_{0101} &= \frac{1}{2}(\mathbf{V}_4 - \mathbf{V}_2)\bullet\mathbf{n}_2 \end{aligned}\right\} \quad (6b)$$

$$\left.\begin{aligned} w_{1010} &= \frac{1}{2}(\mathbf{V}_1 - \mathbf{V}_3)\bullet\mathbf{n}_3 \\ w_{0110} &= \frac{1}{2}(\mathbf{V}_2 - \mathbf{V}_3)\bullet\mathbf{n}_3 \\ w_{0011} &= \frac{1}{2}(\mathbf{V}_4 - \mathbf{V}_3)\bullet\mathbf{n}_3 \end{aligned}\right\} \quad (6c)$$

In Equation 5, the shape of a surface patch is defined by the weights w_{2000}, w_{0200}, w_{0020}, w_{0002}, … w_{0101}, a basic problem in the deformation of a trunctet is to determine the weights of the deformed trunctet. There are altogether nine weights in Equation 5. However, the surface patch always pass through the base vertices $\mathbf{V}_1$, $\mathbf{V}_2$ and $\mathbf{V}_3$ of the trunctet so that the weights at these vertices are zero, i.e. $w_{2000} = w_{0200} = w_{0020} = 0$. Hence, Equation 5 is rewritten as

$$a_b(s,t,u,v) = w_{0002}v^2 + 2w_{1100}st + 2w_{1001}sv + 2w_{0011}uv + 2w_{0110}tu + 2w_{1010}su + 2w_{0101}tv = 0 \quad (7)$$

Without loss of generality, w_{0002} is set to 1. The number of unknowns is thus reduced to 6. Six points on the surface of the deformed trunctet is thus sufficient for determining the deformed surface.

3.1 Locating Surface Points

In order to avoid numerically unstable results, the surface points are chosen so that they are approximately evenly distributed. Six surface points, $\mathbf{p}_1$, $\mathbf{p}_2$, $\mathbf{p}_3$, $\mathbf{q}_1$, $\mathbf{q}_2$ and $\mathbf{q}_3$, where $\mathbf{p}_1$, $\mathbf{p}_2$ and $\mathbf{p}_3$ are surface points on the edges of a trunctet, as shown in Figure 4 are chosen.

Since all surface points are expressed in barycentric coordinates, the corresponding s, t, u and v have to be determined for every surface points. The point $\mathbf{p}_1$ lies on the edge between $\mathbf{V}_1$ and $\mathbf{V}_2$ and is located around the middle of the edge so that $u = 0$ and $t = 0.5$. By substituting $u = 0$ and $t = 0.5$ into the surface equation and the convexity constraint, i.e.

$$\left.\begin{aligned} a_b(s,t,u,v) &= 0 \\ s+t+u+v &= 1 \end{aligned}\right\} \quad (8)$$

the parameters s and v can be evaluated. Similarly, the barycentric coordinates of $\mathbf{p}_2$ and $\mathbf{p}_3$ are obtained.

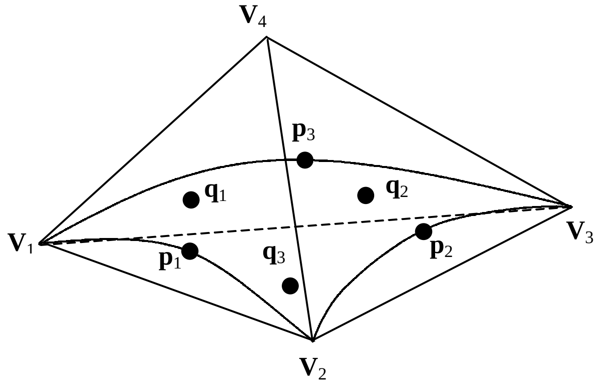

Figure 4 Selection of Surface points

At the surface points $\mathbf{q}_1$, $\mathbf{q}_2$ and $\mathbf{q}_3$, the corresponding s, t, u and v are all non-zero. Those s, t, u, v values are chosen in a way such that $\mathbf{q}_1$, $\mathbf{q}_2$ and $\mathbf{q}_3$ are approximately evenly distributed over the surface. These parameters are chosen as denoted on the base triangle of the construction tetrahedron as shown in Figure 5.

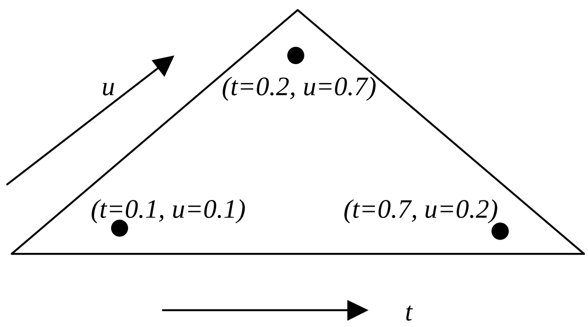

Figure 5 Parameter values of surface points

The barycentric coordinates of $\mathbf{q}_1$ is obtained by assuming $t = 0.1$ and $u = 0.1$ in the surface equation $a_b(s,t,u,v) = 0$ and the convexity constraint $s+t+u+v = 1$. Similarly, the barycentric coordinates of $\mathbf{q}_2$ and $\mathbf{q}_3$ are obtained by setting $t = 0.2$, $u = 0.7$ and $t = 0.7$, $u = 0.2$ respectively.

3.2 Evaluating the Deformed Surface Patch

In a deformation process, the vertices of the trunctet and the surface points in Cartesian coordinates are transformed with a free-form deformation function. By expressing the location of the deformed surface point in the barycentric coordinates of the deformed tetrahedron. The weights of the deformed trunctets are obtained by solving Equation 7.

Assuming the deformed surface points are $\mathbf{p}_1' = (s_1, t_1, u_1, v_1)$, $\mathbf{p}_2' = (s_2, t_2, u_2, v_2)$, $\mathbf{p}_3' = (s_3, t_3, u_3, v_3)$, $\mathbf{q}_1' = (s_4, t_4, u_4, v_4)$, $\mathbf{q}_2' = (s_5, t_5, u_5, v_5)$, and $\mathbf{q}_3' = (s_6, t_6, u_6, v_6)$, the weights of the deformed surface are obtained by

$$\begin{bmatrix} w_{1100} \\ w_{1001} \\ w_{0011} \\ w_{0110} \\ w_{1010} \\ w_{0101} \end{bmatrix} = -\begin{bmatrix} 2s_1t_1 & 2s_1v_1 & 2u_1v_1 & 2t_1u_1 & 2s_1u_1 & 2t_1v_1 \\ 2s_2t_2 & 2s_2v_2 & 2u_2v_2 & 2t_2u_2 & 2s_2u_2 & 2t_2v_2 \\ 2s_3t_3 & 2s_3v_3 & 2u_3v_3 & 2t_3u_3 & 2s_3u_3 & 2t_3v_3 \\ 2s_4t_4 & 2s_4v_4 & 2u_4v_4 & 2t_4u_4 & 2s_4u_4 & 2t_4v_4 \\ 2s_5t_5 & 2s_5v_5 & 2u_5v_5 & 2t_5u_5 & 2s_5u_5 & 2t_5v_5 \\ 2s_6t_6 & 2s_6v_6 & 2u_6v_6 & 2t_6u_6 & 2s_6u_6 & 2t_6v_6 \end{bmatrix}^{-1} \begin{bmatrix} s_1^2 \\ s_2^2 \\ s_3^2 \\ s_4^2 \\ s_5^2 \\ s_6^2 \end{bmatrix}$$

Finally, the normals $\mathbf{n}_{i'}$ at the vertices are determined with the following sets of equations.

$$\mathbf{n}_1' = \begin{bmatrix} (\mathbf{V}_2-\mathbf{V}_1)_x & (\mathbf{V}_2-\mathbf{V}_1)_y & (\mathbf{V}_2-\mathbf{V}_1)_z \\ (\mathbf{V}_3-\mathbf{V}_1)_x & (\mathbf{V}_3-\mathbf{V}_1)_y & (\mathbf{V}_3-\mathbf{V}_1)_z \\ (\mathbf{V}_4-\mathbf{V}_1)_x & (\mathbf{V}_4-\mathbf{V}_1)_y & (\mathbf{V}_4-\mathbf{V}_1)_z \end{bmatrix}^{-1} \begin{bmatrix} w_{1100} \\ w_{1010} \\ w_{1001} \end{bmatrix}$$

$$\mathbf{n}_2' = \begin{bmatrix} (\mathbf{V}_1-\mathbf{V}_2)_x & (\mathbf{V}_1-\mathbf{V}_2)_y & (\mathbf{V}_1-\mathbf{V}_2)_z \\ (\mathbf{V}_3-\mathbf{V}_2)_x & (\mathbf{V}_3-\mathbf{V}_2)_y & (\mathbf{V}_3-\mathbf{V}_2)_z \\ (\mathbf{V}_4-\mathbf{V}_2)_x & (\mathbf{V}_4-\mathbf{V}_2)_y & (\mathbf{V}_4-\mathbf{V}_2)_z \end{bmatrix}^{-1} \begin{bmatrix} w_{1100} \\ w_{0110} \\ w_{0101} \end{bmatrix}$$

$$\mathbf{n}_3' = \begin{bmatrix} (\mathbf{V}_1-\mathbf{V}_3)_x & (\mathbf{V}_1-\mathbf{V}_3)_y & (\mathbf{V}_1-\mathbf{V}_3)_z \\ (\mathbf{V}_2-\mathbf{V}_3)_x & (\mathbf{V}_2-\mathbf{V}_3)_y & (\mathbf{V}_2-\mathbf{V}_3)_z \\ (\mathbf{V}_4-\mathbf{V}_3)_x & (\mathbf{V}_4-\mathbf{V}_3)_y & (\mathbf{V}_4-\mathbf{V}_3)_z \end{bmatrix}^{-1} \begin{bmatrix} w_{1010} \\ w_{0110} \\ w_{0011} \end{bmatrix}$$

4. Outer and Depression Trunctet Transition

In a deformation process, an outer trunctet or part of an outer trunctet may become a depression trunctet or vice versa. It is thus essential to determine if a trunctet changes from an outer to a depression trunctet (or vice versa). Whenever there is a transition, a trunctet vertically opposite the original one has to be used to represent the deformed trunctet (Figure 6a). Based on Equation 6, whether a trunctet changes from an outer to a depression trunctet (or vice versa) can be determined from the sign of the weights w_{1001}, w_{0101} and w_{0011}. Vertices with positive weights w_{1001}, w_{0101} and w_{0011} lie above the surface. The vertices with negative weights w_{1100}, w_{1010} and w_{0110} lie below the surface. A trunctet with all these weights negative is an outer trunctet, whereas a trunctet with all these weights positive is a depression trunctet. If the sign of one of the weights is different from the others, then both an outer and a depression trunctet have to be used (Figure 6b). Whenever a trunctet changes from an outer to a depression trunctet (or vice versa), a depression (or outer) trunctet is constructed by reversing the direction of the normals at the vertices of the base triangle of the trunctet. Similarly, if both an outer and a depression trunctet is to be used, then the additional trunctet is constructed by reversing the direction of the normals at the vertices.

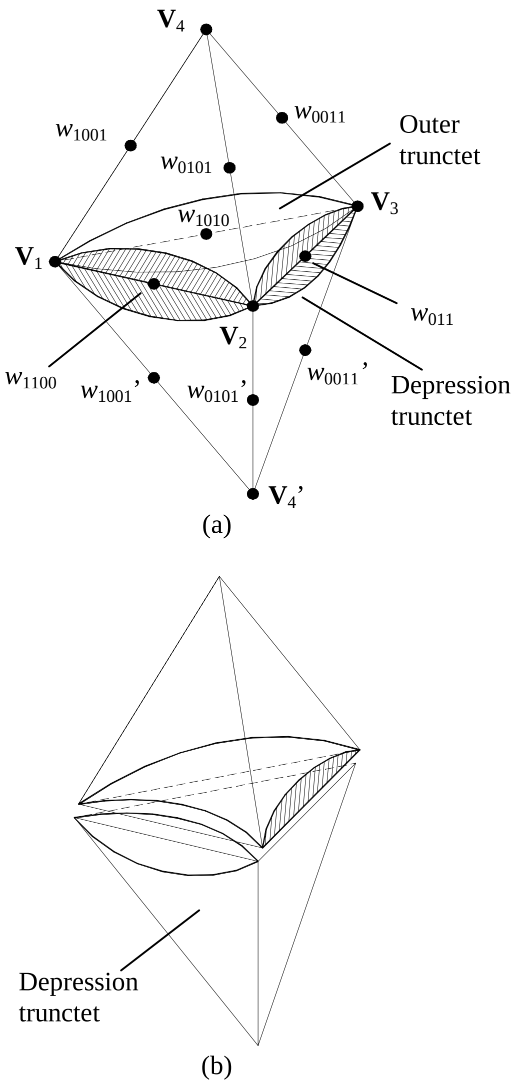

Figure 6 The Outer and Depression Trunctet
(a) Weights and the trunctets
(b) Trunctets with $w_{1010}<0$, $w_{0110}<0$, $w_{1100}>0$

5. Relation between the FFD Lattice and the Trunctets

One characteristic in using FFD for deformation is that the location of the lattice points will affect the possible outcome of the deformation. For example, a ripple shape may be obtained using the lattice in Figure 7a, but not the lattice in Figure 7b.

Since a ripple shape cannot be modeled with a single quadric patch, the lattice points have to be positioned such that no ripple on a single trunctet will be obtained in a deformation. Assume $\mathbf{Q}_a$ and $\mathbf{Q}_b$ are two adjacent lattice points, then the distance between $\mathbf{Q}_a$ and $\mathbf{Q}_b$ must be greater than the distance between two vertices of any trunctets of the model, i.e. $\left|\mathbf{Q}_a - \mathbf{Q}_b\right| \ge \left|\mathbf{V}_i - \mathbf{V}_j\right|$, where $\mathbf{V}_i$, $\mathbf{V}_j$ are vertices of a trunctet. Given a desired lattice, the trunctets of a CSR model thus may have to be subdivided to maintain the above relation.

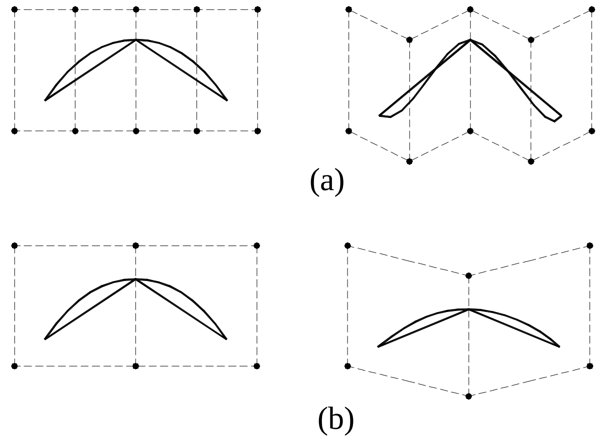

Figure 7 Effect of Lattice Point Distance on the Deformation of Trunctets

6. Implementation

An experimental system was implemented using a CSG geometric kernel *SvLis* [15]. Trunctets in the system are modeled as the intersection of the half-spaces defined by the planes of the tetrahedron and the surface given by Equation 6. Figure 8 shows the deformation of a cylinder. Figure 8b shows the result of deforming the cylinder globally. Figure 8c illustrates the result of a locally deformed cylinder. Figure 9a shows the construction of a toothpaste container. The main body of the container is constructed by applying a freeform deformation on the cylinder shown in Figure 8. The container is further deformed using FFD giving the result of Figure 9b. Figure 10 shows the result of deforming a thick circular disk followed by subtracting a rectangular block from the deformed disk.

7. Conclusion

This paper presented an approach for deforming solid models represented in CSR. An object is constructed by subtracting depression trunctets from the union of outer trunctets and the polyhedron core. Deforming a CSR solid is to evaluate the deformed polyhedron core and trunctets. The deformed polyhedron core is obtained by deforming the vertices of the polyhedron. Trunctets are deformed by a surface fitting approach. Six approximately evenly distributed points on a trunctet of the object are used to define the quadric patch of the trunctet. By expressing these points in barycentric coordinates of the defining tetrahedron, weights defining the trunctet can be evaluated. Applying free-form deformation on these points allows the surface of a deformed trunctet to be evaluated. Tests on an experimental system showed that the approach is promising and is capable of generating complex freeform solid objects using freeform deformation.

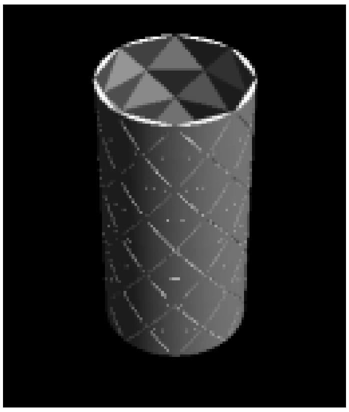

(a)

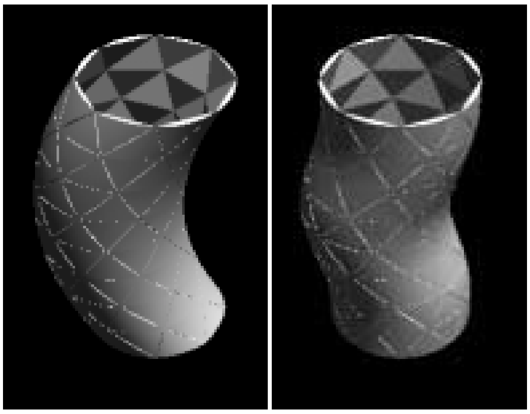

(b) (c)

Figure 8 Deformation of a cylinder model
(a) The undeformed cylinder
(b) The globally deformed cylinder
(c) The localy deformed cylinder

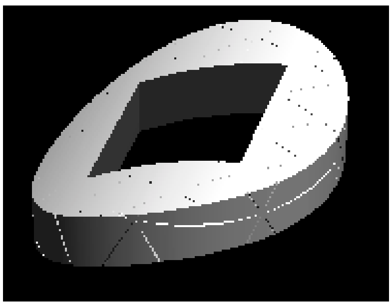

Figure 10 A deformed disk with a rectangular through hole

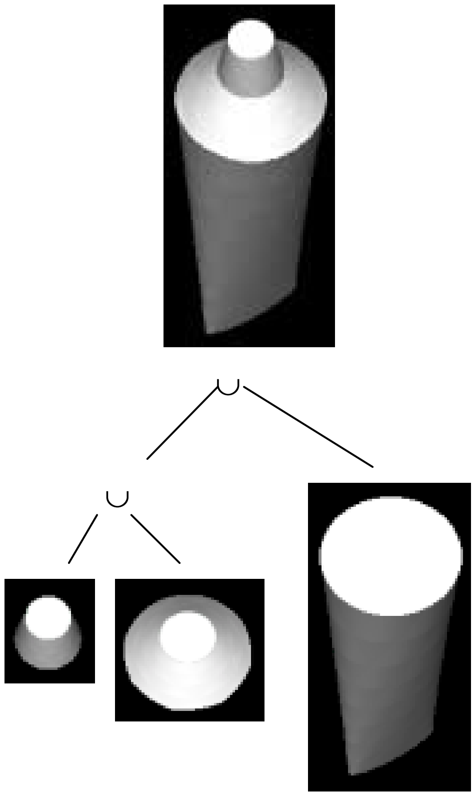

(a)

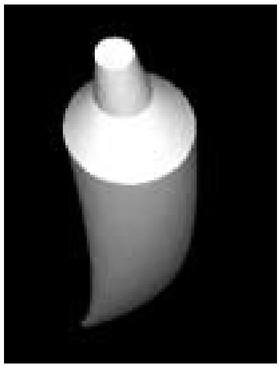

(b)

Figure 9 A toothpaste container
(a) The construction of a toothpaste container
(b) The deformed container

Acknowledgement

This work is partially supported by a Direct Grant (ID 2050231) of the Chinese University of Hong Kong.

References

1. T. W. Sederberg and S. R. Parry, "Free-Form Deformation of Solid Geometric Models", *ACM Computer Graphics (Proc. of SIGGRAPH '86)*, 20(4), 151-160, 1986.

2. S. Coquillart, "Extended free-form deformation: A sculpturing tool for 3D geometric modeling", *ACM Computer Graphics (SIGGRAPH '90)*, 24(4), 187-196, 1990.
3. P. Kalra, A. Mangili, N. M. Thalmann, and D. Thalmann., "Simulation of facial muscle actions based on rational free-form deformation", *Computer Graphic Forum (Eurographics'92 Proc.),* 2(3), C59-C69, 1992

4. H. Lamousin and W. Waggenspack, "NURBS-Based Free-Form Deformations", *IEEE Computer Graphics and Applications*, 14(9):59-65, 1994

5. P. Faloutsos, M. Panne and D. Terzopoulos, "Dynamic Free-Form Deformations for Animation Synthesis", *IEEE Transactions on Visualization and Computer Graphics*, 3(3):201-214, 1997.

6. H. B. Voelcker, "New Directions in Solid Modeling ?", *Proc. International Conference on Manufacturing Automation*, 1992, pp. 157-168.

7. H. Chiyokura and F. Kimura, "Design of solids with free-form surfaces", *ACM Computer Graphics (SIGGRAPH '83)*, 17(3):289-298, 1983.

8. J. Alander, M. Mantyla and T. Rantanen, "Solid modeling with parametric surfaces", *Proc. of Eurographics'83*, pp. 71-83, 1983.

9. M. S. Castle, "Free-form solid modeling with trimmed surfaces", *IEEE Computer Graphics and Applications*, pp. 33-43, January 1987.
10. R.F. Sarraga and W. C. Waters, "Free-form surfaces in GMSOLID: goals and issues", *Solid Modelling by Computers: From Theory to Applications*, Penum Press, USA, pp. 237-258, 1984.

11. K. C. Chan, *Solid Modelling of Parts with Quadric and Free-form Surfaces*, Ph.D. dissertation, University of Hong Kong, 1987.

12. A. Dunnington, D. R. Saia, and A. de Pennington, "Constructive solid geometry with sculptured primitives using inner and outer sets", in Strasser, W and Seidal H P (Eds) *Theory and Practice of Geometric Modelling,* Springer-Verlag, pp. 127-142, 1989.

13. J.P. Menon, *Constructive Shell Representations*, Technical Report CPA92-5, The Sibley School of Mechanical and Aerospace Engineering, Cornell University, 1992.

14. G. Baining, *Modeling Arbitrary Smooth Objects with Algebraic Surfaces*, Ph.D Thesis, Department of Computer Science, Cornell University, 1991.

15. Adrian Bowyer, *SvLis – Introduction and User Manual*. 1994.